Proceedings of the
9th Graz Brain-Computer Interface Conference 2024

10.3217/978-3-99161-014-4-025

DETECTION OF MOTION TERMINATION FROM EEG DURING THE EXECUTION OF CONTINUOUS HAND MOVEMENT

Markus Crell[1], Gernot R. Müller-Putz[1,2]

[1]Institute of Neural Engineering, Graz University of Technology, Graz, Austria

[2]BioTechMed Graz, Graz, Austria

E-mail: gernot.meuller@tugraz.at

ABSTRACT: Recent advances in the decoding of hand kinematics from neural data and the usage for the control of cursors also prompt the need to detect the begin and end of continuous movements. This study investigates the asynchronous detection of the termination of a continuous hand movement in a handwriting task using electroencephalography data and the power of frequencies in the μ and β band. Results obtained with a shrinkage linear discriminant analysis classifier yield a correct determination of the offset in 53.5% (chance level: $\approx$ 18%) of the trials. We show the general feasibility of the proposed method in the detection of the termination of a continuous hand movement and visualize the benefit of the information of the moment of movement termination in a simulated application.

INTRODUCTION

Communication capabilities for patients using brain-computer-interfaces (BCIs) have recently been greatly enhanced through the decoding of continuous motion from neural data during imagined hand movements [1]. For people in the late stages of amyotrophic lateral sclerosis (ALS) or with any form of locked-in syndrome, such methods can provide highly desirable ways for the interaction with the outside world [2]. Although most improvements have been driven by advances in implantable devices and the resulting improvement of signal quality [1], non-invasive BCIs employing electroencephalography (EEG) have lately shown promising advances in the field of continuous movement decoding [3] and could potentially be adopted in a comparable way in the future. An important aspect of the decoding of continuous movement and the reconstruction of hand trajectories for the usage in cursor control is the discontinuation of the movement. For imperfect control, as is to be expected at the current state of continuous movement decoding, trajectories have to be constantly corrected by the user [4]. While this can be acceptable during the execution of controlling the cursor where users are engaged with the task, unintended movement should be avoided during periods in which patients are not engaged with the cursor control and where an incessantly moving cursor could be irritating. One way of overcoming this problem is the detection of voluntary movement initiation and termination and the utilization for starting and stopping of the cursor control. The execution of movement is accompanied by different neural phenomena of which mostly the movement-related cortical potential (MRCP) and event-related de-/synchronization (ERD/ERS) have received major attention. While MRCPs [5] are detectable directly in the time-series EEG and are time- and phase-locked to the start of the movement [6], oscillatory components (ERD) in μ and β frequencies decrease during planning and execution of a movement until the motion is terminated [7, 8]. At the point of termination, the desynchronization is followed by a period of increased β synchronization before returning to the baseline, also known as post-movement β synchronization (in short β *rebound*). ERD and ERS are phenomena which are typically observed in μ and β frequencies of the EEG and have been extensively studied for different movement tasks. While a large body of research has focused on the detection of movement onsets [6, 9, 10], few studies have explored the detection of movement termination. Only limited work examined the usage of ERD/ERS patterns for the termination of movement imagination of single, short foot dorsiflexion [11, 12]. They showed that the classification of the β-ERS patterns proved more reliable and resulted in a higher detection accuracy for the imagined movement. Hortal et al. reported similar classification accuracies for the detection of start and stop of the gait cycle from μ and β frequency power [13]. In a related approach, Bai et al. employed β-ERS to classify repetitive imagined and executed wrist movement [14]. They reported overall high discriminability between execution and termination and better performance in the execution case than for imagination. Noticeably, the mentioned studies used either short single or repetitive movements. More recently, Orset et al. investigated the detection of termination of sustained movement imagination of the hand, achieving an accuracy of 76.2% [15]. While these studies form a basis for the detection of discontinuation of movements as needed for the stop of cursor control from EEG, they do not integrate the self-initiation of the termination of a continuous movement as is inherent to the control of a

Published by
Verlag der Technischen Universität Graz

10.3217/978-3-99161-014-4-025

computer cursor.

We aimed to detect the movement termination (herein termed *offset* in contrast to the *onset* of a movement) of a continuous and autonomously executed hand motion. We designed a paradigm in which participants were tasked with the writing of letter trajectories, which constitute a continuous hand and finger movement. Although the movement onset was defined based on a cue, the stop of the motion was dependent on the letter itself as well as on the speed and size of the writing trajectory, which varied among participants and over the duration of the paradigm.

MATERIALS AND METHODS

Experimental Paradigm: The study was conducted among 22 healthy, right-handed participants with a mean age of 27.5 ± 3.92 years (mean $\pm$ standard deviation). Each subject participated in a paradigm with an approximate duration of 2.5 h. Participants were fitted with an EEG cap equipped with 60 electrodes which were placed on the head according to a standard 10-10 EEG montage. Four electrodes were positioned on the outer canthi of the eyes as well as above and below the left eye to measure electrooculogram (EOG) signals induced by eye movements. The experiment consisted of (1) an instruction phase during which participants were informed about the measurement and the paradigm, (2) a measurement of specified eye movements for the elimination of eye artifacts in EEG data and (3) the execution of a session of the paradigm. Steps 2 and 3 were repeated twice and separated by a break of approximately 10-20 min. The specified eye movements were part of the SGEYESUB algorithm and are described further in [16]. One session of the paradigm contained seven (first session) and eight (second session) runs separated by breaks of 60 s. During each run 40 trials were performed in each of which one out of 10 letters (*a,d,e,f,j,n,o,s,t,v*) was written with the index finger of the right hand. Finger movements were recorded with a custom motion capture algorithm tracking a visual marker applied to the right index finger of the participant. During trials, participants observed a screen and waited for a letter to fade onto the screen (duration: 2 s), stay on the screen at full opacity (0.5 s) and fade out again (2 s). As soon as the letter was invisible, participants started to write the displayed letter with their finger and stopped at the last point of the letter without any further movement. The maximum duration of writing a letter was limited to 4 s, after which the next letter would be faded onto the screen. Every letter was written 60 times, resulting in a total of 600 executed movements. Due to technical problems and early termination, two participants had to be excluded from the study.

Data Acquisition and Preprocessing: EEG was acquired from two biosignal amplifiers (BrainAmp, Brain Products GmbH, Germany) at a sampling rate of 500 Hz. The signals were bandpass-filtered between 0.3-70 Hz and Notch-filtered at 50 Hz to eliminate powerline noise. Eye artifacts were removed using the SGEYESUB algorithm [16] and signals from the EOG channels. Residual eye and muscle artifacts were removed by applying independent component analysis. The EEG was finally re-referenced using a Laplacian reference and 24 channels on the outer periphery of the montage including the EOG channels were removed from the dataset. We further extracted the start and stop of the motion from the movement data using the falling and rising edge of the trajectory speed. The kinematic data was recorded at 30 Hz and smoothed with a Savitzky-Golay filter (first order polynomials and window length of 200 ms).

Neural Correlates of Movement Termination: An analysis of the neural correlates of the offset of continuous movements was conducted using ERD/ERS patterns. 20 frequency bands between 0.3 and 40 Hz were extracted using Morlet wavelets [17]. The data was split into trials of length $[-2.5; 4.0]s$ relative to (a) the start of the movement or (b) the stop of the movement. We then extracted the relative change in power of the time-frequency data A to the reference period R, in this case the whole trial [7].

$$ERD/ERS\% = \frac{A-R}{R} * 100\% \quad (1)$$

Finally, the trials were averaged aligned according to (a) and (b) for each channel. We additionally examined the delay between movement onset and offset from the kinematics to compare with the spread of ERD/ERS patterns when aligned to the onset of the movement.

Movement Offset Detection: Detection of the movement offset was implemented by classifying windows of neural data into *movement* and *no movement* and determining the falling edge. We extracted time-frequency data around six center frequencies ($8, 12, 16, 20, 24$ and 28 Hz) using Morlet wavelets to cover the range of μ and β frequency bands. We obtained the slow changes in power, equivalent to the envelope of the signal, of specific frequency bands by lowpass filtering the band-filtered data to 12 Hz and subsequently downsampled the features to 30 Hz to reduce the amount of data. The relative change in frequency power was calculated according to Eq. 1 with the reference period set to $[-2.5; 0]$s relative to the movement onset. The trials were then cut to include the time period $[0.2, 4.0]s$ relative to the start of the movement. Trials in which the offset of the movement happened more than 4 s after the cue onset were discarded. The data was then labeled as *movement* until the movement offset and as *no movement* between the movement offset and the end of the trial. Windows of length w_L between $[t_0 - w_L; t_0]$ were created to classify the label at $t_0 - lag$ with a lag of $\frac{w_L}{2}$ to incorporate non-causal information for the classification. (see Fig. 1a). t_0 was shifted with a stride of one sample to generate the labeled data. A 5-fold cross-validation procedure was employed and a shrinkage linear discriminant analysis was used for the classification. For each participant, a separate model was trained and evaluated. After training the models, windows were classified sequentially per trial to retain the order and allow for a reconstruction of the labeling per trial from the classified data. We then defined

Published by
Verlag der Technischen Universität Graz

10.3217/978-3-99161-014-4-025

a detection strategy for the definition of movement offsets from the classified data by generating the majority vote from five consecutive classifications and choosing the first falling edge as movement offset after which the subsequent ten samples (i.e. ≈ 330ms) were successively classified as *no movement*. For each trial, a movement offset was defined as correctly identified when the detected offset was within a range of ±330 ms of the actual offset. Since the window length of each trial was 3.8 s, the chance level for a random classifier was approximately 18% with a level of statistical significance of 21.1% calculated according to [18]. We tested window sizes of $w_L \in [200, 400, 500, 600, 800] ms$ and a lag of $\frac{w_L}{2}$.

Simulated Application - Handwritten Letters: To visualize the benefit of the information of the moment of termination of the continuous movement, we employed a simulated application in which handwritten letters were classified from reconstructed trajectories. We simulated imperfect reconstruction of trajectories from neural data by adding noise to the measured x and y positions obtained during the handwriting task. The noise, derived from lowpass-filtered white Gaussian noise, ranged from zero to a maximum amplitude of 1.5 times the average letter size. We then constructed windows of 4 s starting from the movement onset and constructed images of the handwritten trajectory. This procedure was executed for different conditions:

- NN: **N**o additional **n**oise was added to the recorded trajectories and the full four second window was used for the image construction.
- AN: **A**dditional **n**oise as described above was applied to the trajectories and the full four second window of noisy trajectory data was used for the image construction.
- AN-C: **A**dditional **n**oise as described above was applied to the trajectories, which were **c**ut after the movement offset, and only the shortened window was used for the image construction.
- AN-P: **A**dditional **n**oise as described above was applied to the trajectories, which were cut after the movement offset according to the **p**redictions from the classifier, and only the shortened window was used for the image construction.

These conditions are visualized in Fig. 1b. A convolutional neural network (CNN) for the detection of handwritten letters from images was employed to classify the constructed letters. CNNs are often utilized in the recognition of handwritten characters since they have proven to yield high accuracies [19]. We repeated a 5-fold cross validation procedure twice to generate reliable classification results.

RESULTS

Neural Correlates of Movement Termination: An analysis of the lag between movement onset and offset per trial showed that the average movement was terminated after 1.9 s with a standard deviation of 0.6 s. We also investigated the difference between movement onset and offset for individual letters with the distribution shown in Fig. 2a. The largest difference in the average duration of movements between letters occurred for letters *d* (2.44 ± 0.62s) and *v* (1.33 ± 0.43s). We also found an influence of the writing duration on the distribution since the coefficient of variation increased with longer average duration of the letters (Pearson's r: 0.73, p-value: 0.017). We then calculated the ERD/ERS maps for the movement onset (Fig. 2b upper images) and movement offset (Fig. 2b lower images) aligned trials. Desynchronization (relative decrease of power in the frequencies) is shown in red while synchronization (relative increase of power in the frequencies) is shown in blue. Movement onset centered ERD/ERS maps are also overlayed with an aligned distribution map of the movement offset to indicate the moment of termination of the writing motion. An ERD in μ and β frequencies during the movement and a post-movement β synchronization can be observed. Furthermore, a μ-ERS can be observed, however, delayed to the β-ERS. Those patterns are more pronounced at channel C1, contralateral to the movement of the right finger.

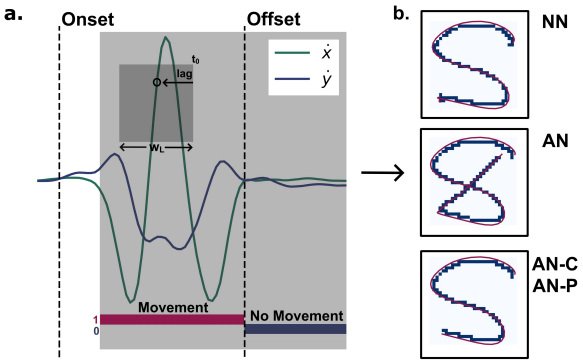

Figure 1: (a) Schematic of the movement kinematics used for the detection of onset and offset and the labeling of the data for the classification. Labels are chosen 200 ms after the movement onset until 4 s after the movement onset and are classified from frequency data of length w_L using a lag to incorporate non-causal information. (b) The illustration shows letters reconstructed from kinematics and transformed into an image for classification using a CNN. Letters are shown for the conditions no-noise (**NN**), additional-noise (**AN**) and additional-noise-cut (**AN-C/AN-P**).

Movement Offset Detection: The maximum accuracy for the detection of movement offsets was achieved for a window length of $w_L = 500$ ms with an average accuracy of $53.3 \pm 11.9\%$ (mean ± standard deviation) over all participants. The subject with the best performance reached an accuracy of 77.5%. Average classification accuracies achieved with different window lengths yielded lower but comparable results ($49.9 \pm 13.0\%$, $53.2 \pm 12.4\%$, $52.7 \pm 12.0\%$, $51.4 \pm 11.0\%$ for window sizes 200, 400, 600 and 800 ms, respectively). For all participants, the classification accuracy was above chance. The influence of the

Published by
Verlag der Technischen Universität Graz

10.3217/978-3-99161-014-4-025

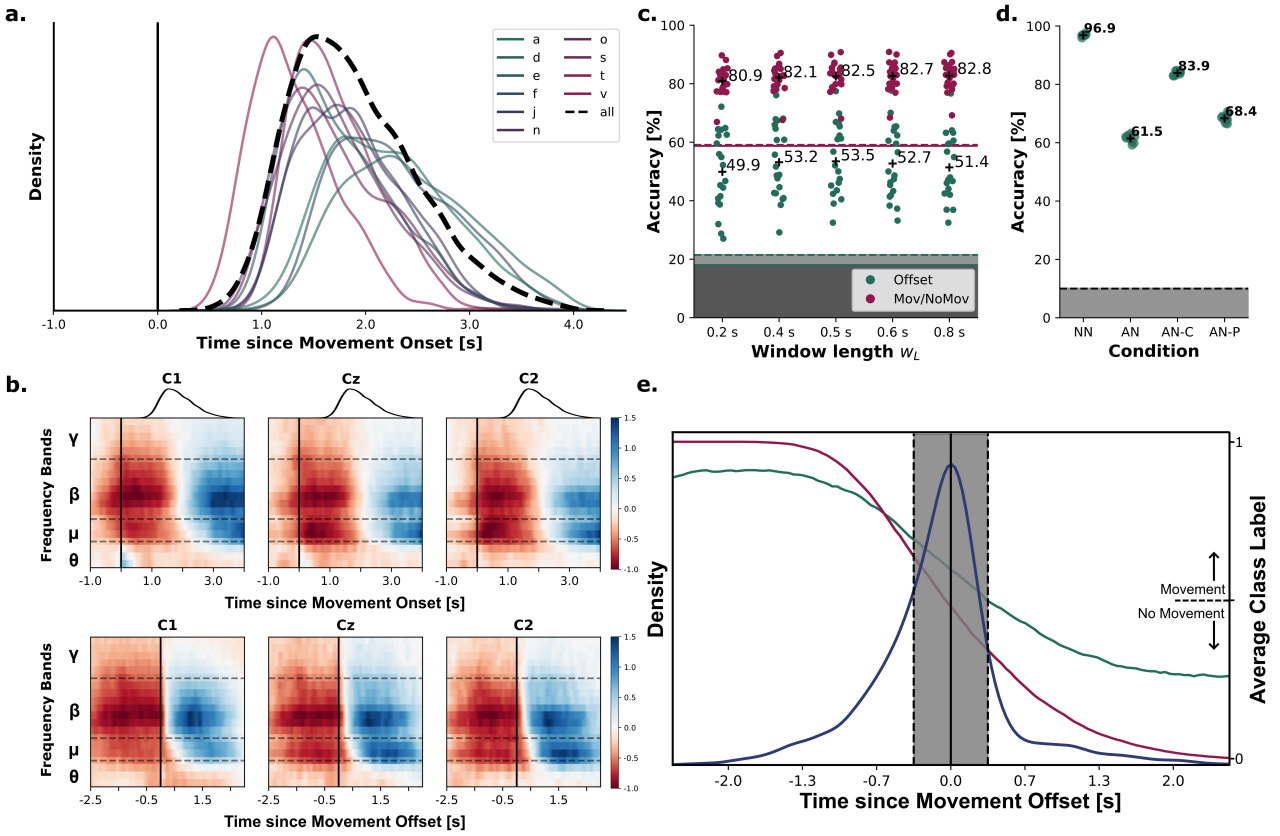

Figure 2: (a) Density plot of the distribution of the movement offset of the handwritten letters relative to the start of the movement. The distributions for the ten individual letters are shown together with the overall distribution. (b) ERD/ERS maps of electrodes C1, Cz and C2 for frequency bands aligned to the movement onset (upper plots) and movement offset (lower plots). Black straight lines indicate the movement onset/offset while dashed lines indicate the frequency band borders. (c) Classification accuracies for the detection of the movement onset (green) and classification between *movement* and *no movement* (red) for the different window lengths. Results for the individual subjects are plotted as dots, average results are marked by a cross. Theoretical and statistical chance levels for both classifications are indicated by lines in the corresponding color. (d) Results for the simulated application of classifying handwritten letters under different conditions of noise and length of the kinematic trajectories. (e) The density plot for the detected movement offsets displaying the difference between actual and detected movement offset per trial is shown in blue. The image also depicts the average predicted class of *movement* or *no movement* in green and the actual average class in red.

window length w_L was not significant ($p > 0.05$) between window lengths 200-800 ms, 400-500 ms and 400-600 ms as assessed with a paired t-test. The density distribution for the temporal difference between actual and detected movement offset is shown in Fig. 2e in blue. The grey area displays the time range around the actual offset in which detected offsets were considered to be correct. This area contains 53.5% of the detected offsets, the area to the left contains 24.8% and the area to the right 10.9%. In 10.8% of the trials, no movement offset was detected. When increasing the threshold for considering a predicted offset to be correct to ± 500 ms, the accuracy could be increased to 64.3%. We also analyzed the binary classification accuracy for the classification of *movement* vs. *no movement*, which acted as a basis for the detection of the movement offset. The highest accuracy was achieved for a window length of $w_L = 800$ ms with an average accuracy of $82.8 \pm 4.8\%$ over all participants. The best performance of a single participant was achieved for the same subject as in the offset detection at an accuracy of 90.5%. The average classification accuracies for different window lengths were $80.9 \pm 4.8\%$, $82.1 \pm 4.9\%$, $82.5 \pm 4.9\%$, $82.7 \pm 4.9\%$ for window sizes $200, 400, 500$ and 600 ms, respectively. The average class label over the trials is shown in Fig. 2e in green (actual class label) and red (predicted class label). The probability for a prediction of movement at the beginning of a trial was 0.92 (actual probability: 1.0) and 0.25 (actual probability: 0.0) at the end of a trial. Results for all subjects are shown in Fig. 2c in green for the offset detection and in red for the classification between *movement* and *no movement*.

Simulated Application - Handwritten Letters: Handwritten letters could be correctly classified from the recorded kinematics with an average accuracy of 96.9% over all subjects in the **NN** condition in which no additive noise was applied and the trajectories were not cut at the movement offset. When additive noise was applied to the trajectories (**AN** condition) the classification accuracy

Published by
Verlag der Technischen Universität Graz

10.3217/978-3-99161-014-4-025

dropped to 61.5%. Cutting the noisy trajectories after the actual movement offset (**AN-C** condition) increased the accuracy to 83.9%. The usage of the detected motion offset for cutting the noisy trajectories (**AN-P** condition) enabled an increase of the classification accuracy by 6.9% compared to the **AN** condition and achieved a total accuracy of 68.4%. The results of the 2-times repeated 5-fold cross-validation are shown in Fig. 2d.

DISCUSSION

Continuous decoding of hand movement, especially in EEG, stands to benefit from the detection of movement offsets. So far, the limited research in this area showed promising results [11–15]. We attempted the detection of the movement offset from time-frequency data after continuous movement and obtained a moderate accuracy of 53.5% against a chance level of 21.1%. We also showed the benefit of including this information into an exemplary application of classification of handwritten letters.

Neural Correlates of Movement Termination: The constructed ERD/ERS maps show the connection of the desynchronization in μ and β frequencies with the continuous movement as well as the synchronization in these frequencies as soon as the movement terminates. The ERD/ERS maps exhibit broader distribution and reduced intensity of synchronization when trials are aligned to movement onset compared to alignment with movement offset. This is caused by the time-locking of the synchronization to the termination of the movement and the dispersion of the movement offset as shown in Fig. 2a. These findings are also in accordance with literature [7, 8, 20, 21]. The dependency of frequency power on the movement on- and offset generally shows that a classification of *movement* vs. *no movement* based on the time-frequency data is possible. Since the effects are mostly occurring in the μ and β frequencies, the usage of these frequencies is appropriate.

Movement Offset Detection: The maximum average accuracy of 53.5% is comparable to those achieved in other movement offset detection BCIs [11, 13]. The classification accuracy of around 82% for the binary classification is also in the range of performances of similar BCIs [22]. Interestingly, the accuracies for different subjects were more dispersed in the detection of the movement offset than for the underlying binary classification. Also, the influence of the window length proved to be different for the detection of the movement offset and the binary classification with an optimal window length of 500 ms for the offset detection and an increasing accuracy of the classification with longer window lengths. It is possible that these differences occurred due to the decision strategy with which movement offsets were defined being suboptimal for some participants. A closer analysis of the distribution of *movement* vs. *no movement* classifications might yield insight into this and allow for the formulation of a better strategy. The distribution of differences between detected and actual movement offsets as given in Fig. 2e shows a tendency of predicting the movement offset earlier than the actual offset. This could similarly be influenced by the detection strategy, which used the first feasible predicted offset as the detected offset and discarded every other following feasible offset. Since the *movement* vs. *no movement* classification is imperfect, this strategy naturally leads to a higher rate of false positives in the beginning than at the end of a trial. Due to the non-causal window length and the detection strategy requiring ten continuous predictions being classified as *no movement*, the causal latency between a detected and actual movement offset amounts to 580 ms. Including the range of $\pm$ 330 ms in which the detected offset was considered correct, the minimal and maximal latency between stating a correctly detected and actual offset is between 250 and 910 ms. This calculation also shows that shorter window lengths should generally be preferred to longer ones in order to minimize the latency. Since the drop in detection performance proved to be limited for shorter window lengths in this study, other studies that employ a similar paradigm online should consider choosing a short window length for the classification.

Simulated Application - Handwritten Letters: The increase in classification accuracy of the **AN-C** and **AN-P** conditions compared to the **AN** condition in the simulated handwritten letter classification task shows the positive influence of the inclusion of motion termination information. While the actual movement offset information generated an increase of 22.4%, the offsets detected from neural data still allowed for an increase of 6.9%. Although this increase is modest, it demonstrates that classifiers also benefit from the inclusion of the moment of movement termination for imperfect detection performances. While the slight increase in accuracy compared to the **AN-C** condition might be improved by increasing the accuracy of the offset detection, other methods could also be effective: since the movement offset tended to be predicted earlier than the actual offset, we tested a modification in which all offsets predicted before 1.5 s after the movement onset were set to 1.5 s. With this method, we were able to increase the classification accuracy in the **AN-P** condition to 72.6% (i.e., an increase of 11.1% compared to **AN**). Other, more sophisticated approaches could increase the accuracy even further. It needs to be noticed that the simulated additive noise might not be representative of the distortion of movements in real-world decoding of hand trajectories from neural data. The benefit of the movement offset inclusion under the influence of different noise must be evaluated depending on the actual task at hand. However, in cases where the distortion leads to a residual, erroneous motion after the actual offset, the additional detection of the movement termination and incorporation of this information can be of great use.

CONCLUSION

This study showed the general feasibility and benefit of the detection of self-initiated movement offsets during

Published by
Verlag der Technischen Universität Graz

10.3217/978-3-99161-014-4-025

continuous hand motion. While the accuracy of the detection was modest, it showed that detection is generally possible with a low latency. We also proved that a movement offset detection can be useful to increase the accuracy in specific movement-related tasks even for limited performance of the detection model. Since the benefit of including the movement termination detection grows with its accuracy, we aim to enhance the performance in the future. Recently, a new method for the detection of *movement* vs. *no movement* classes has been proposed using a pole tracking algorithm [23]. Although this method has not yet been applied to EEG, it could pose a way of increasing the classification and detection performances. While the current study focused on the detection of self-initiated motion termination, the start of the movements was based on an external cue, which prevented the application of a classifier to identify both movement onset and offset. Future work should focus on self-paced continuous movement tasks to investigate the detection of both start and end of continuous movements.

ACKNOWLEDGEMENTS

This project is funded by the European Union's HORIZON-EIC-2021-PATHFINDER CHALLENGES program under grant agreement No 101070939 and by the Swiss State Secretariat for Education, Research and Innovation (SERI) under contract number 22.00198.

REFERENCES

[1] Willett FR, Avansino DT, Hochberg LR, Henderson JM, Shenoy KV. High-performance brain-to-text communication via handwriting. Nature. 2021;593(7858):249–254.
[2] Vansteensel MJ *et al.* Towards clinical application of implantable brain–computer interfaces for people with late-stage ALS: medical and ethical considerations. Journal of Neurology. 2023;270(3):1323–1336.
[3] Mondini V, Kobler RJ, Sburlea AI, Müller-Putz GR. Continuous low-frequency EEG decoding of arm movement for closed-loop, natural control of a robotic arm. Journal of Neural Engineering. 2020;17(4):046031.
[4] Pulferer HS, Kostoglou K, Müller-Putz GR. Getting off track: Cortical feedback processing network modulated by continuous error signal during target-feedback mismatch. NeuroImage. 2023;274:120144.
[5] Shibasaki H, Hallett M. What is the Bereitschaftspotential? Clinical Neurophysiology. 2006;117(11):2341–2356.
[6] Pereira J, Kobler R, Ofner P, Schwarz A, Müller-Putz GR. Online detection of movement during natural and self-initiated reach-and-grasp actions from EEG signals. Journal of Neural Engineering. 2021;18(4):046095.
[7] Pfurtscheller G, Silva FLd. Event-related EEG/MEG synchronization and desynchronization: basic principles. Clinical Neurophysiology. 1999;110(11):1842–1857.
[8] Pfurtscheller G, Brunner C, Schlögl A, Silva FLd. Mu rhythm (de)synchronization and EEG single-trial classification of different motor imagery tasks. NeuroImage. 2006;31(1):153–159.
[9] Liu D *et al.* EEG-Based Lower-Limb Movement Onset Decoding: Continuous Classification and Asynchronous Detection. IEEE Transactions on Neural Systems and Rehabilitation Engineering. 2018;26(8):1626–1635.
[10] Müller-Putz GR, Scherer R, Pfurtscheller G, Rupp R. EEG-based neuroprosthesis control: A step towards clinical practice. Neuroscience Letters. 2005;382(1-2):169–174.
[11] Pfurtscheller G, Solis-Escalante T. Could the beta rebound in the EEG be suitable to realize a "brain switch"? Clinical Neurophysiology. 2009;120(1):24–29.
[12] Müller-Putz GR, Kaiser V, Solis-Escalante T, Pfurtscheller G. Fast set-up asynchronous brain-switch based on detection of foot motor imagery in 1-channel EEG. Medical & Biological Engineering & Computing. 2010;48(3):229–233.
[13] Hortal E, Úbeda A, Iáñez E, Azorín JM, Fernández E. EEG-Based Detection of Starting and Stopping During Gait Cycle. International Journal of Neural Systems. 2016;26(07):1650029.
[14] Bai O, Lin P, Vorbach S, Floeter MK, Hattori N, Hallett M. A high performance sensorimotor beta rhythm-based brain–computer interface associated with human natural motor behavior. Journal of Neural Engineering. 2008;5(1):24.
[15] Orset B, Lee K, Chavarriaga R, Millán JdR. User Adaptation to Closed-Loop Decoding of Motor Imagery Termination. IEEE Transactions on Biomedical Engineering. 2019;68(1):3–10.
[16] Kobler RJ, Sburlea AI, Lopes-Dias C, Schwarz A, Hirata M, Müller-Putz GR. Corneo-retinal-dipole and eyelid-related eye artifacts can be corrected offline and online in electroencephalographic and magnetoencephalographic signals. NeuroImage. 2020;218:117000.
[17] Morlet Wavelets and Wavelet Convolution. In: Analyzing Neural Time Series Data: Theory and Practice. The MIT Press, Jan. 2014.
[18] Müller-Putz G, Scherer R, Brunner C, Leeb R, Pfurtscheller G. Better than random? a closer look on bci results. International Journal of Bioelectromagnetism. 2008;10(1):52–55.
[19] Baldominos A, Saez Y, Isasi P. A Survey of Handwritten Character Recognition with MNIST and EMNIST. Applied Sciences. 2019;9(15):3169.
[20] Müller G, Neuper C, Rupp R, Keinrath C, Gerner H, Pfurtscheller G. Event-related beta EEG changes during wrist movements induced by functional electrical stimulation of forearm muscles in man. Neuroscience Letters. 2003;340(2):143–147.
[21] Seeber M, Scherer R, Müller-Putz GR. EEG Oscillations Are Modulated in Different Behavior-Related Networks during Rhythmic Finger Movements. The Journal of Neuroscience. 2016;36(46):11671–11681.
[22] Rashid M *et al.* Current Status, Challenges, and Possible Solutions of EEG-Based Brain-Computer Interface: A Comprehensive Review. Frontiers in Neurorobotics. 2020;14:25.
[23] Müller-Putz G, Crell M, Egger J, Suwandjieff P, Kostoglou K. Towards Implantable Brain-Computer Interface for Communication in Locked-In Syndrome patients. Current Directions in Biomedical Engineering. 2023;9(2):1–4.

Published by
Verlag der Technischen Universität Graz